Journal of Applied Electrochemistry (2024) 54:1299–1307
https://doi.org/10.1007/s10800-023-02028-1

RESEARCH ARTICLE

Electrochemical synthesis and characterization of zinc sulfide (ZnS) semiconducting thin films from citrate-based plating bath

Meriem Hamla[1,2] · Mohamed Benaicha[2] · Yazid Chetbani[3] · Oualid Dilmi[2]

Received: 27 July 2023 / Accepted: 4 November 2023 / Published online: 22 November 2023

Abstract

The primary purpose of this article is to synthesize electrochemically a binary semiconductor material ZnS that is generally used for manufacturing solar cells. It has been shown that the properties and composition of the deposits are closely linked to the synthesis conditions, namely the applied potential, the electrolyte concentration and its composition. The electrodeposition was realized from an acidic medium with a pH ranging from 3.5 to 4.5 and containing respectively 0.02 M of zinc chloride ($ZnCl_2$), 0.02 M of sodium thiosulphate ($Na_2S_2O_3$), and 0.15 M of trisodium citrate ($Na_3C_6H_5O_7$) as complexing agent. The deposition mechanism of ZnS binary alloys was investigated using various electrochemical techniques. ZnS thin films were electrochemically deposited on a tin-doped indium oxide (ITO) substrate in one single step, at a potential of −1 V/SCE. The effects of the concentration ratio ([zinc]/[sulfur]) on the electrochemical, optical, and compositional properties of thin films as well as their surface morphology were also investigated.

Graphical abstract

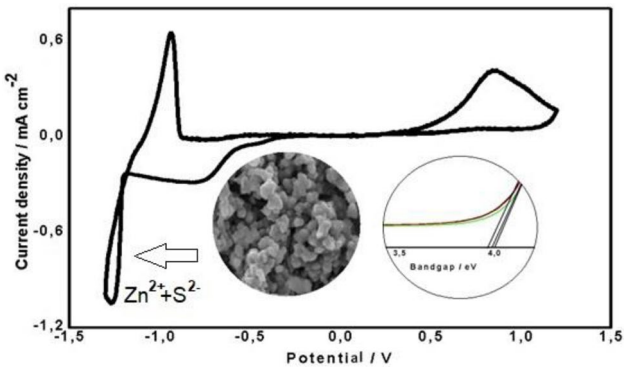

Keywords Electrodeposition · Thin films · Zinc sulfide · Solar cells · Semiconductor · Band gap

✉ Meriem Hamla
meriem.hamla@univ-bba.dz

[1] Department of Matter Sciences, Faculty of Science and Technology, University Mohamed El Bachir El Ibrahimi of Bordj Bou Arréridj, 34030 El Anceur, Algeria

[2] Energetics and Solid-State Electrochemistry Laboratory (ESEL), Department of Processes Engineering, Faculty of Technology, Ferhat Abbas-Sétif 1 University, 19000 Sétif, Algeria

[3] Laboratory of Mechanics and Materials Development, Department of Civil Engineering, Faculty of Science and Technology, University of Djelfa, 17000 Djelfa, Algeria

1 Introduction

Over the past few decades, solar energy has increasingly been viewed as the most promising renewable energy source. Indeed, the sun is considered as the energy source of the future due to its abundance and inexhaustible character. It is worth emphasizing that the main factors to be considered when producing new materials for solar cell applications are the band gap energy that corresponds to the solar spectrum, and the cost of production [1].

In the recent past, heterojunction solar cells have received much attention from researchers in the field of solar energy. Among the photovoltaic materials of recent interest, one may mention the low-cost and non-toxic chalcogenides, such as ZnS [2] and SnS. Zinc sulfide (ZnS) is a (II-VI) semiconductor compound of major importance; it has a wide direct forbidden band of 3,68 eV [3]. In addition, this material possesses a broad optical transparency ranging from ultraviolet (UV) to infrared (IR) [4]. This optical transparency coupled with the chemical and thermal stability makes ZnS one of the most widely used materials as a window layer in heterojunction photovoltaic solar cells. Zinc sulfide is one of the most important group II-VI optical semiconductor materials. Considering its unique physico-chemical properties, this compound has been receiving increasing attention due to a wide variety of potential applications in optoelectronic devices, such as the ultraviolet light-emitting diodes, efficient thin-film phosphors for electroluminescent devices [5], and other optoelectronic devices like the electroluminescent displays, cathodoluminescent displays, and multilayer dielectric filters [6–9], in addition to anti-reflective coatings for heterojunction solar cells [10, 11].

It is worth highlighting that ZnS nanostructures have been synthesized using various techniques, including the chemical bath deposition [12–14], atomic layer deposition [15], RF reactive sputtering [16], thermal evaporation [17, 18], spray pyrolysis [19–22], and electrodeposition [23, 24]. Moreover, it has been widely revealed that the electrodeposition technique is the most promising process for the preparation of thin films, as it offers the possibility of large-scale production, simple deposition process monitoring, and easy control of deposition parameters [25, 26].

Recently, much research work has been done to study the electroplating process. In this regard, Benyahia et al. [27] used an elaboration strategy that is based on the combination of the vacuum thermal evaporation technique and oxidation process, under an annealing temperature of 500 °C, to prepare the ZnO–ZnS compound. The results showed a compound exhibiting a fairly dense structure with the properties of a granulated surface without pinholes. In addition, void regions were visible at the top surface, with a quite high visible absorbance capacity that is superior to 62%. Moreover, the band gap found (2.65 eV) was smaller than that of the ZnS film that was fabricated via the evaporation method (3.4 eV). On the other hand, Azmand et al. [28] adopted an electrochemical method to synthesize Al-doped ZnS thin films from $AlCl_3$ plating bath on Indium Tin Oxide (ITO) substrates. They suggested that Al doping decreases the crystallite size of ZnS samples and increases their dislocation density and lattice strain. Similarly, UV–Vis spectroscopy showed that Al doping decreases the band gap energy of ZnS samples from 3.93 to 3.50 eV. In this regard, Mosavi et al. [29] electrodeposited Cd-doped ZnS nanostructures from a $CdCl_2$ electrolyte and reported that introducing the Cd dopant reduced the ZnS film band gap energy from 3.95 eV to 3.63 eV as a result of the presence of imperfections and crystal disorders in the Cd-doped ZnS samples. As for Boosagulla et al. [30], they fabricated zinc sulphide (ZnS) thin films via the pulsed electrodeposition technique using organic reagents, without subsequent heat treatment of the samples. They suggested that the layers obtained by a combination of glycerol and tartaric acid produced a good quality ZnS compound, with a band gap energy of 3.8 eV, as has been confirmed by the X-ray diffraction (XRD), micro-Raman and optical investigations. With regard to Kassim et al. [01], they reported the deposition of zinc sulfide (ZnS) thin films, under potentiostatic regime, from an aqueous solution, at room temperature. They then concluded that the electrolysis at −1.1 Volts vs. SCE electrode, for a period of 30 min, was sufficient for the preparation of ZnS thin films with a cubic crystalline phase.

In the present work, ZnS thin films were deposited in one step on ITO substrates, at room temperature, in an aqueous plating bath containing trisodium citrate as a complexing agent, using the cost-effective pulsed electrodeposition technique without the heat treatment step. The effects of deposition potential (Ed) and concentration ratios ([zinc]/[sulfur]) on the morphology and phase composition of ZnS deposits were studied using, respectively, the UV–visible technique, field emission scanning electron microscopy (FESEM), energy dispersive X-ray spectroscopy (EDS) and the X-ray diffraction (XRD) technique as well.

2 Experimental

The electrolytes used for the electrodeposition of the ZnS thin films consisted of an aqueous solution containing 0.02 M $ZnCl_2$ and 0.02 M $Na_2S_2O_3$. In addition, the trisodium citrate ($C_6H_5Na_3O_7$) was used as a complexing agent and hydrochloric acid (HCl) as a pH control solution. The pH was set within a range between 3.5 and 4.5.

The experimental device used was a standard three-electrode cell, with a platinum substrate having an area of 0.5 cm^2 as the working electrode, a platinum (Pt) electrode as the counter-electrode, and a saturated calomel electrode (SCE) as a reference electrode. This device was used for the electrochemical study of chemical species. Additionally, the working electrode was chemically polished using a nitric acid solution.

For the electrodeposition of thin ZnS layers, the ITO (indium tin oxide) working electrode, with a surface of (1×2) cm^2, was used. The quality of the deposit and that of the sample both depend on the cleanliness and the state of the ITO substrate surface, which means that the substrate cleaning is a step of major importance. In this case, all

traces of grease and dust must be removed, and the surface of the substrate must be visually checked for any scratches or unevenness. It is important to emphasize that these conditions are essential for good adhesion of the deposit to the substrate, and also for its uniformity (constant and uniform thickness). Before each measurement, the ITO substrates must first be degreased with acetone for a period of about 5 min, and then well rinsed with distilled water.

They are next immersed in nitric acid (HNO_3) for a few seconds. Then, upon activation of the ITO substrates by the acid, the H^+ ions can create electroactive sites on the SnO_2 surface in order to make the electrodeposition process simpler. It is important to mention that the ITO substrates contain only one electroactive face (SnO_2 doped In) on which the electrochemical reaction can take place, while the other face is completely isolated (glass only). Therefore, the acid treatment of substrates used for electrodeposition may affect one face only. A longer chemical treatment could create microscopic irregularities on the ITO surface that, in turn, could tune the film growth morphology. It is worth emphasizing that the same time was taken for the chemical treatment of all ITO substrates which were rinsed again with distilled water, and finally dried and cleaned with optical paper.

The electrochemical experiments were carried out using a potentiostat/galvanostat (Voltalab PGZ 301) that was monitored by a microcomputer. All experiments were performed under constant temperature conditions (T = 25 °C). Cyclic voltammetry was used to study the electrochemical behavior of ZnS on a Pt substrate and also to choose the most appropriate deposition potential. The optical study, in the UV–visible domain on ITO substrate, was carried out in order to determine the value of the band gap energy of the material obtained. In addition, the surface microstructure and composition of the ZnS alloy were also investigated using a field emission scanning electron microscope (FE-SEM, JEOL JSM-7100 F) that was equipped with an energy dispersive spectrometer (EDS) working under a 20 kV accelerating voltage. The X-ray diffraction (XRD) patterns of the (ZnS/ITO) thin layers were recorded on an X-ray diffractometer (Philips X'Pert Pro) that is suplied with a Cu-Kα radiation source (λKα = 1,5418 Å).

3 Results and discussion

3.1 Cyclic voltammetry

The stability domain of the supporting electrolyte is an important feature when studying any electrochemical system. Figure 1 shows a typical voltamperogram of the electrolyte solution in an electrolytic bath that contains 0.15 M $Na_3C_6H_5O_7$. In the absence of active ions (Zn^{2+}, S^{2-}), there

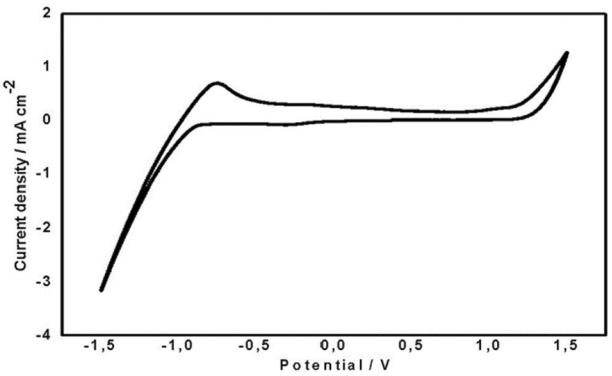

Fig. 1 Voltamperogram relative to the Pt substrate immersed in a solution containing 0.15 M sodium citrate ($Na_3C_6H_5O_7$), with a scanning speed of 10 mV s^{-1}

are two currents, i.e., a cathodic current and an anodic current at the ends of a wide domain of inactivity that ranges from − 0.8 to + 1 V/SCE. It should be noted that a cathodic current, which was attributed to the release of hydrogen, was observed at a potential around − 0.8 V/SCE. In addition, it was noticed that oxygen was released beyond the potential + 1 V/ECS.

Prior to moving to the ZnS binary alloy, a study, using cyclic voltammetry on Pt substrate in baths containing Zn^{2+} and S^{2-} ions, was deemed necessary. Figure 2 shows the cyclic voltamperograms of Zn^{2+} and S^{2-} ions in separate baths, recorded on the working electrode, at the scan rate of 10 mV s^{-1}. With regard to the zinc solution (Fig. 2a), a reduction peak of Zn^{2+} ions ($Zn^{2+} + 2e^- \rightarrow Zn$), centered at −0.65 V/SCE, appeared. For more electronegative potentials, the current density increase reflects the evolution of hydrogen. However, by reversing the direction of scanning, a single peak, located at −0.06 V/SCE, appeared in the anodic part, which corresponds to the dissolution peak of Zn $\left(Zn \rightarrow Zn^{2+} + 2e^-\right)$ already formed during scanning, followed by passivation.

With regard to the sulfur solution (Fig. 2b), the cathodic section consists of a peak that corresponds to the reduction of sulfur ions ($S_2O_3^{-2} + 6H^+ + 4e^- \rightarrow 2S + 3H_2O$ *and* $S_2O_3^{-2} \rightarrow S + SO_3^{-2}$) and is located at −0.82 V/SCE, in addition to an increase in current density as a consequence of the hydrogen evolution reaction. By reversing the scanning direction, a single peak, located at + 0.93 V/SCE, appeared in the anode part, which corresponds to the dissolution peak of sulfur ($S_2O_3^{-2} + 3H_2O \rightarrow 2H_2SO_3 + 2H^+ + 4e^-$), as previously observed during the forward scan.

With regard to the ZnS binary alloy, the cyclic voltammetry curve was plotted between the stationary potential 1.5 V/SCE and − 1.5 V/SCE, as is illustrated in Fig. 3. During the cathode scanning, a small cathode current was observed at the potential of −0.44 V/SCE. Then,

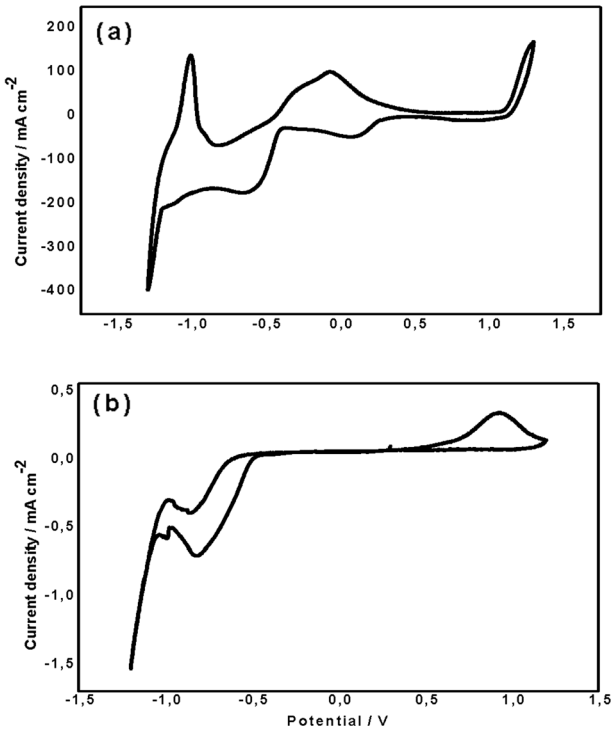

Fig. 2 Voltamperograms relative to the Pt substrate immersed in a solution containing 0.15 M of $Na_3C_6H_5O_7$ with the addition of (0.02 M $ZnCl_2$, $2H_2O$) for (**a**), and (0.02 M $Na_2S_2O_3$, $5H_2O$) for (**b**), with a scan rate of 10 mV s^{-1}, and a pH equal to 4.2

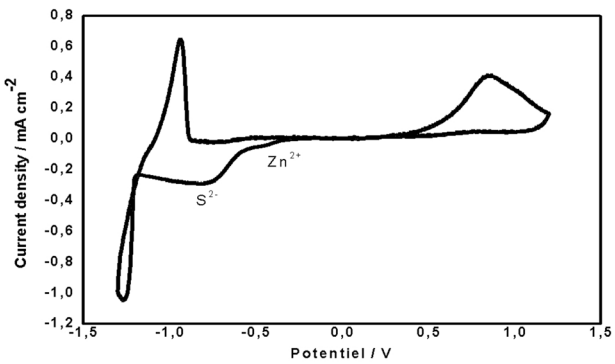

Fig. 3 Voltamperogram relating to the Pt substrate that is immersed in a solution containing 0.15 M $Na_3C_6H_5O_7$, 0.02 M ($Na_2S_2O_3$, $5H_2O$) and 0.02 M ($ZnCl_2$, $2H_2O$), with a scanning rate of 10 mV s^{-1}, at pH = 4.2

the current increased sharply to a potential of −0.78 V/SCE. By comparison with the previous curves depicted in Fig. 2 a, b, it is clear that these two peaks correspond to the reduction of Zn and S. Further, the reverse scan shows two other peaks, centered at −0.95 V/SCE and + 0.86 V/SCE, resulting from the electrodissolution of the ZnS deposit.

The ZnS deposition takes place in accordance with the following overall reaction:

$$Zn^{2+} + S_2O_3^{-2} + 2e^- \rightarrow ZnS + SO_3^{-2} \quad (1)$$

The plot of the current density as a function of potential, at different scanning rates (v = 10, 20, 40, 60, and 80 mV s^{-1}) within the potential range that extends from 1.5 to −1.5 V/SCE, is depicted in Fig. 4 a, b, and c, for Zn, S, and ZnS, respectively. It is worth noting that as the scanning speed increases, the peaks become wider and their potentials undergo a shift. The evolution of the characteristic parameter of the voltammogram (Ip) as a function of the scanning

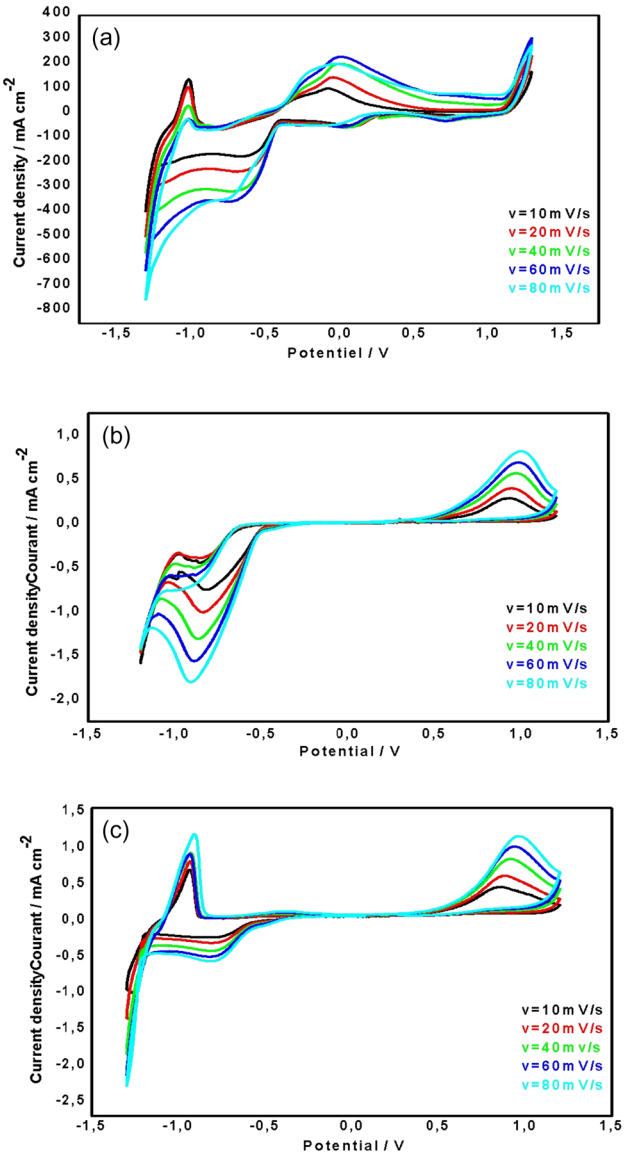

Fig. 4 Voltamperograms obtained at different scan rates, for: **a** Zn, **b** S, and **c** ZnS, on the Pt substrate, at pH = 4.2

speed makes it possible to notice the redox behavior at the electrode.

The electrolyte solution used is composed of 0.02 M $Na_2S_2O_3$, 0.02 M $ZnCl_2$, and 0.15 M $Na_3C_6H_5O_7$, for a pH equal to 4.2, for the respective metals Zn, S, and ZnS on the Pt substrate. It was revealed that the cathodic peak current (i_{pc}) varies linearly with the square root of the scan rate ($v^{1/2}$), as shown in Fig. 5b, d and f. Likewise, the cathodic peak potential (E_{pc}) varies linearly with the logarithm of the scan rate (*log v*), with positive slopes (Fig. 5a, c, and e). This clearly indicates that the deposition reaction is controlled by the diffusion [31, 32]. Furthermore, it was observed that the higher the imposed scanning rate, the greater the density of the reduction current of the ions Zn^{2+} and S^{2-}.

Figure 6 shows the voltamperograms obtained from an electrolytic solution containing 0.02 M $Na_2S_2O_3$, 0.02 M $ZnCl_2$, and 0.15 M $Na_3C_6H_5O_7$, at pH = 4.2. The curves plotted correspond to the Pt substrate, for a scanning speed equal to 10 mV/s, and for the three ratios $R_{0.25}$, R_1, and R_5, as summarized in Table 1, for the binary alloy ZnS. These same curves clearly indicate that the intensity of the reduction and oxidation peaks, in both systems, is directly dependent on the bath concentration, so that each time the sulfur concentration increases, the peaks become more intense. In

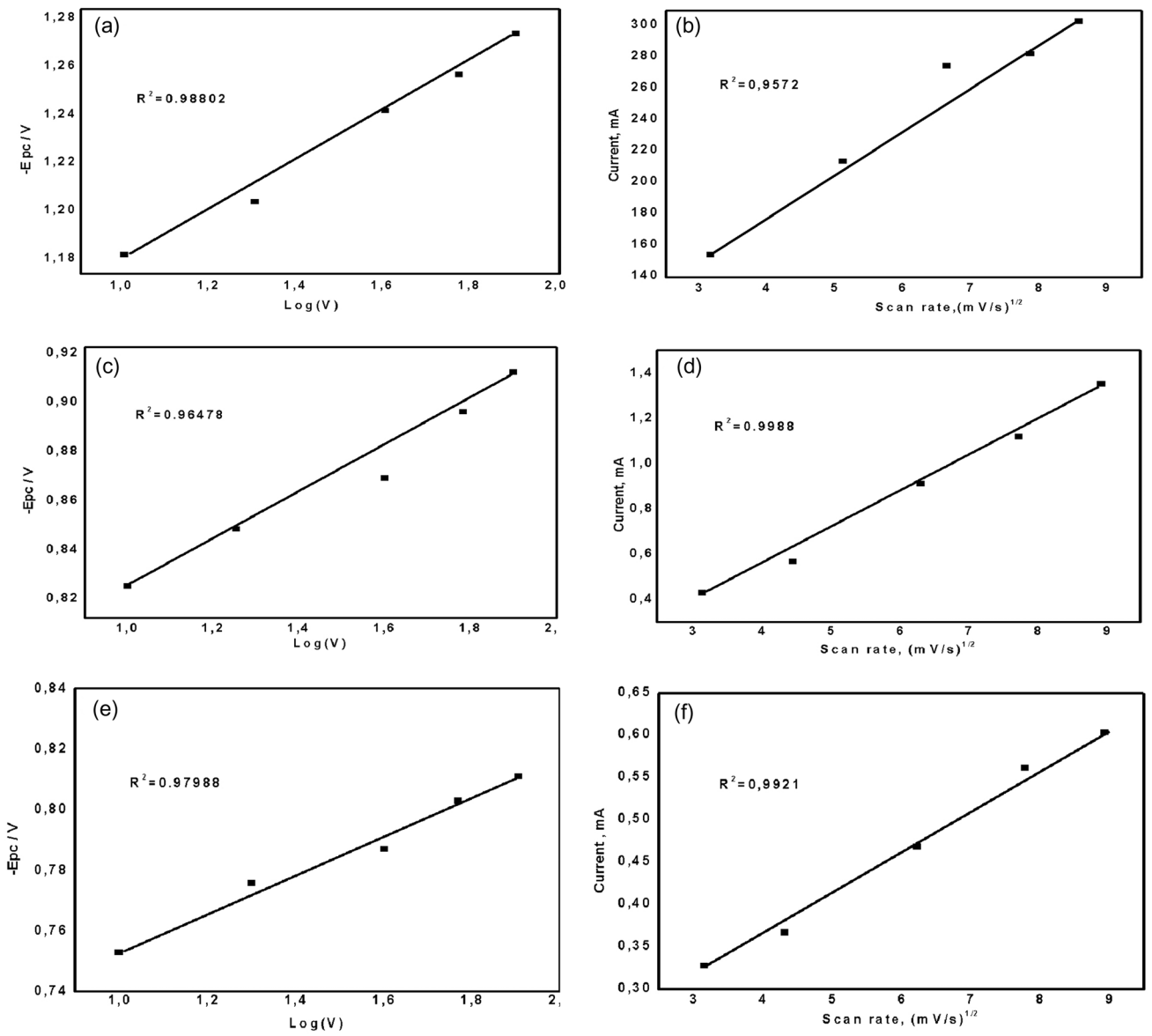

Fig. 5 Variation of the cathode peak intensity (i_{pc}) as a function of the square root of the scan rate ($v^{1/2}$) and variation of cathode peak potential (E_{pc}) as a function of the logarithm of the scan rate (*log v*), for the electrodeposition of Zn (**a**, **b**), S (**c**, **d**), and ZnS (**e**, **f**), on the Pt substrate, at pH = 4.2

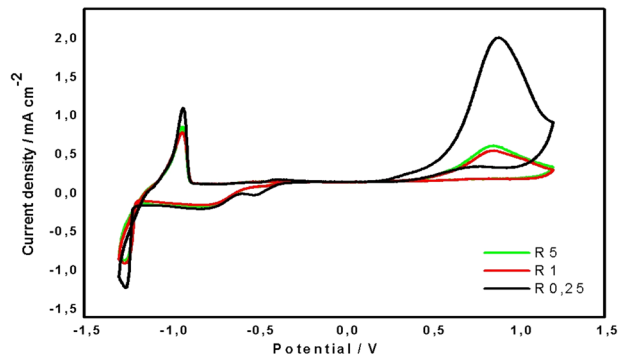

Fig. 6 Cyclic voltammograms obtained at different ratios, i.e., $R_{0.25}$, R_1, and R_5, for the binary ZnS alloy, at pH = 4.2

Table 1 Zinc-to-sulfur concentration ratios

	Ratio	Concentration
$R_{0.25}$	R= [Zn]/[S] = 0.25	[25mM] / [100mM]
R_1	R= [Zn]/[S] = 1	[20mM] / [20mM]
R_5	R= [Zn]/[S] = 5	[100mM] / [20mM]

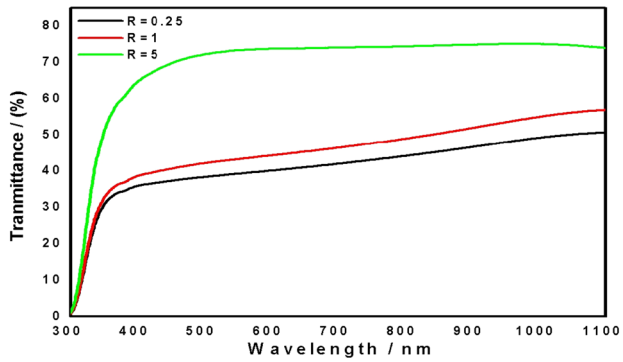

Fig. 7 Optical transmittance spectra of the ZnS thin layers deposited at −1 V/ SCE, under different concentration ratios $R_{0.25}$, R_1, and R_5, on the ITO substrate, during 30 min

other words, the peaks become more intense with decreasing ratios.

3.2 Optical characterization

The most important aspect of thin film characterization lies in the study of its optical properties such as transmittance, band gap energy, activation energy, and others. It should be noted that, in the present case, it was decided to use the method of extrapolation from the graph representing the variation of $(\alpha h\nu)^2$ as a function of $h\nu$, for the ZnS thin layer, in order to determine the band gap energy.

Figure 7 shows typical transmittance spectra of ZnS thin films, recorded within the wavelength range between 300

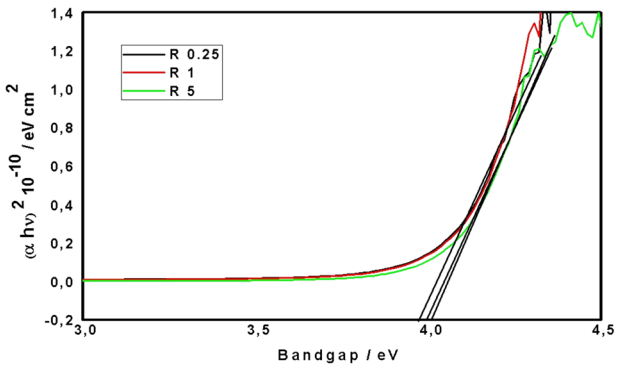

Fig. 8 Band gap energy of the ZnS thin layers deposited at −1 V/ SCE, under different concentration ratios $R_{0.25}$, R_1, and R_5, on the ITO substrate during 30 min, with the plot $(\alpha h\nu)^2$ vs. $(h\nu)$

and 1100 nm, for films deposited at − 1 V/ SCE, under different concentration ratios, i.e., $R_{0.25}$, R_1, and R_5, on the ITO substrate, for a period of 30 min. The curves shown in Fig. 7 allow noticing the presence of a high transparency region ($\lambda > 400$ nm), with a maximum transmission rate of 70%, for ratio R_5. This figure also indicates that the transmittance of ZnS films decreases as the concentration ratios go down. Therefore, the band gap energy can be determined from the plot of $(\alpha h\nu)^2$ as a function of energy $h\nu$ (Tauc-Davis plot) by extrapolating the linear part of the curve that represents the onset of absorption at the intersection with the energy axis.

Likewise, the plots depicted in Fig. 8 suggest that the optical band gap energy of the layers deposited at −1 V decreased from 3.97 to 3.90 eV when the concentration ratios went down. These findings are in good agreement with those reported in the literature [28, 29, 33]. The reaction that can possibly occur during the formation of ZnS thin films can be simplified and expressed in the form:

$$Zn^{2+} + S^{2-} \rightarrow ZnS \quad (2)$$

3.3 Surface morphology investigation

Figure 9 shows the scanning electron microscopy (SEM) images of ZnS thin films deposited at −1 V/SCE, on copper substrate, during 30 min, for the ratio R_1, at different magnifications. It is seen that the deposited film is uniform, whitish, and well covered by the substrate. It is seen that, generally, its surface presents granular-looking layers with diversified morphology and homogeneously distributed grains.

The chemical composition of the ZnS surface was qualitatively and quantitatively analyzed. The EDS results, together with the typical EDS spectrum of the sample that

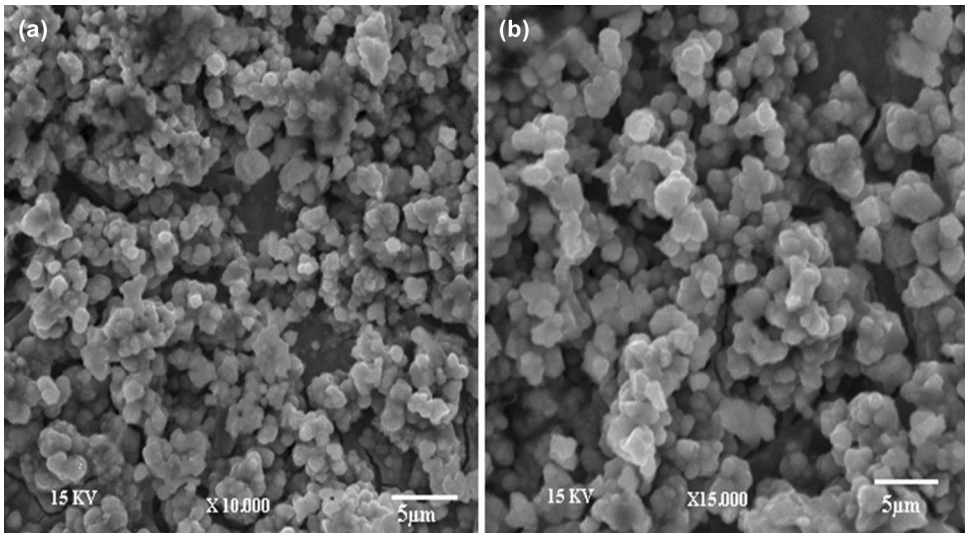

Fig. 9 SEM images of ZnS layers deposited at −1 V/SCE on the copper substrate during 30 min

Fig. 10 EDS spectra of ZnS layers deposited at −1, 0 V vs.SCE, on the copper substrate, at room temperature, for t = 30 min

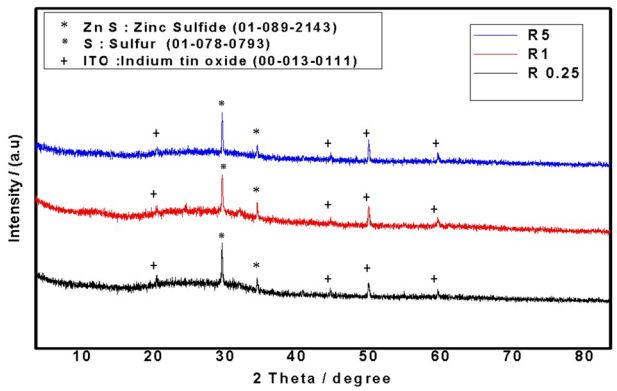

Fig. 11 X-ray diffraction patterns of the ZnS layers deposited at −1 V/SCE, under different concentration ratios ($R_{0.25}$, R_1, and R_5), at pH = 4.2, at room temperature, for 30 min

was deposited at −1 V/SCE on the copper substrate, are shown in Fig. 10. It is noticed that the surface is mainly composed of Zn (32,2%) and S (12,2%). The Zn and S peaks confirm the formation of the ZnS phase. The other peaks, corresponding to Cu (16,5%), C (27,2%), and O (11,9%), are attributed to the copper substrate.

3.4 X-ray diffraction analysis

Figure 11 illustrates the X-ray diffraction spectra of the ZnS thin layer deposited at −1 V/SCE on the ITO substrate, under different concentration ratios ($R_{0.25}$, R_1, and R_5), at room temperature, for a period of 30 min.

The results of the XRD analysis, as depicted in Fig. 11, reveal the presence of the cubic ZnS phase (JCPDS No. 01-089-2143), with a peak located at $2\theta = 33{,}87°$, corresponding to the plane (200), for all the concentration ratios ($R_{0.25}$, R_1, and R_5) considered in this study. Similar findings have been reported in the literature [29, 34].

It should also be noted that peaks attributed to the ITO substrate (00-013-0111) and sulfur (01-078-0793) were also observed for each concentration ratio, at various diffraction angles, i.e., $2\theta = 20{,}86°$, 29,99°, 45,01°, 50,31°, and 59,78°. The results suggest that the presence of sulfur in the sample is associated with the ZnS peaks, which implies that the thin films may contain excess elemental S.

4 Conclusion

The present work aims primarily to study the synthesis of a binary compound that is used as a precursor in ZnS-based solar cells. For this, it was deemed necessary to analyze the electrochemical behavior of the individual zinc and sulfur systems, and then that of the ZnS binary compound.

The study conducted by cyclic voltammetry of the individual systems Zn, S and the binary ZnS compound made it possible to determine the potential of the electrodeposition potentials of each element as well as that of the binary alloy. In addition, it was found that the change in scan rate confirms that the deposition reaction is diffusion controlled. Furthermore, the study of the effect of concentration on the ZnS system, for the three ratios $R_{0.25}$, R_1, and R_5, showed that the size of the reduction and oxidation peaks is directly dependent on the sulfur concentration used. It was indeed found that these peaks become more intense as the sulfur concentration increases, indicating that elemental S is in excess.

The structural, morphological, and optical studies showed that the ZnS thin films deposited at −1 V, for a period of 30 min, for the ratio R_1, exhibited the best results. The optical study, conducted within the visible range between 300 and 1100 nm, indicated that the thin films obtained had a band gap energy of 3.90 eV, with a lower value for the ratio R_1. Moreover, the SEM images showed a homogeneous morphology, with granular surface properties. The EDS spectra also confirmed the formation of the ZnS phase. In addition, the XRD diagrams revealed that all the samples showed a cubic ZnS phase, corresponding to the plane (200).

Acknowledgements The authors wish to acknowledge the financial support from the Algerian Ministry of Higher Education and the Faculty of Science and Technology at Mohamed El Bachir El Ibrahimi University in the city of Bordj Bou Arréridj - Algeria.

Author contributions MH is presently working as a research at the Department of Matter Sciences at the Faculty of Science and Technology, University of Bordj Bou Arréridj, Algeria. She played role in data curation, formal analysis, investigation and writing—original draft preparation. MB contributed to supervision, validation, review and editing. OD contributed to experimentation and investigation. YCH contributed to experimentation and investigation.

Declarations

Conflict of interest The authors declare that there is no conflict of interest related the present work. They have no known competing financial interests or personal relationships that could have appeared to influence the work reported in this paper.

References

1. Kassim A, Nagalingam S, Min HS, Karrim N (2010) XRD and AFM studies of ZnS thin films produced by electrodeposition method. Arab J Chem 3:243–249. https://doi.org/10.1016/j.arabjc.2010.05.002
2. Choi YI, Lee S, Kim SK et al (2016) Fabrication of ZnO, ZnS, Ag-ZnS, and Au-ZnS microspheres for photocatalytic activities, CO oxidation and 2-hydroxyterephthalic acid synthesis. J Alloys Compd 675:46–56. https://doi.org/10.1016/j.jallcom.2016.03.070
3. ÜZAR N, ARIKAN MÇ (2011) Synthesis and investigation of optical properties of ZnS nanostructures. Bull Mater Sci 34:287–292. https://doi.org/10.1007/s12034-011-0085-5
4. Fang X, Zhai T, Gautam UK et al (2011) ZnS nanostructures: from synthesis to applications. Prog Mater Sci 56:175–287. https://doi.org/10.1016/j.pmatsci.2010.10.001
5. Popa M, Zakhidov A, Tiginyanu I (2018) Perovskite solar cells with ZnS as electron transport layer. Proc Romanian Acad Ser -Math Phys Tech Sci Inf Sci 19:559–566
6. Kumar V, Sharma M, Gaur J, Sharma T (2008) Polycrystalline ZnS thin films by screen printing method and its characterization. Chalcogenide Lett 5:289–295
7. Mach R, Müller GO (1982) Physical concepts of high-field, thin-film electroluminescence devices. Phys Status Solidi A 69:11–66
8. Ledger AM (1979) Inhomogeneous interface laser mirror coatings. Appl Opt 18:2979–2989
9. Jones PL, Moore DM, Smith SC (1976) A new method for melting and recrystallization of lanthanum ZnS nanoparticle. J Phys E 9:312–316
10. Jadhav UM, Shinde MS, Patel SN, Patil RS (2014) Structural, optical and electrical properties of nanocrystalline cadmium sulphide thin films deposited by novel chemical route. Indian J Pure Appl Phys 52:39–43
11. Kumar V, Manickam D, Venkatachalam M et al (2007) Structural and Optical Properties of Hydrothermally Grown Zns Thin Films. Int J Innov Res Sci Eng Technol 3297:2319–8753
12. Sartale SD, Sankapal BR, Lux-Steiner M, Ennaoui A (2005) Preparation of Nanocrystalline ZnS by a new chemical bath deposition route. Thin Solid Films 480–481:168–172. https://doi.org/10.1016/j.tsf.2004.11.054
13. Roy P, Ota JR, Srivastava SK (2006) Crystalline ZnS thin films by chemical bath deposition method and its characterization. Thin Solid Films 515:1912–1917. https://doi.org/10.1016/j.tsf.2006.07.035
14. Lădar M, Popovici E-J, Baldea I et al (2007) Studies on chemical bath deposited zinc sulphide thin films with special optical properties. J Alloys Compd 434–435:697–700. https://doi.org/10.1016/j.jallcom.2006.08.226
15. Gunasekaran M, Gopalakrishnan R, Ramasamy P (2004) Deposition of ZnS thin films by photochemical deposition technique. Mater Lett 58:67–70. https://doi.org/10.1016/S0167-577X(03)00416-6
16. Shao L-X, Chang K-H, Hwang H-L (2003) Zinc sulfide thin films deposited by RF reactive sputtering for photovoltaic applications. Appl Surf Sci 212–213:305–310. https://doi.org/10.1016/S0169-4332(03)00085-0
17. Durrani SMA, Al-Shukri AM, Iob A, Khawaja EE (2000) Optical constants of zinc sulfide films determined from transmittance measurements. Thin Solid Films 379:199–202. https://doi.org/10.1016/S0040-6090(00)01539-X
18. Dimitrova V, Tate J (2000) Synthesis and characterization of some ZnS-based thin film phosphors for electroluminescent device applications. Thin Solid Films 365:134–138. https://doi.org/10.1016/S0040-6090(99)01089-5
19. Afifi HH, Mahmoud SA, Ashour A (1995) Structural study of ZnS thin films prepared by spray pyrolysis. Thin Solid Films 263:248–251. https://doi.org/10.1016/0040-6090(95)06565-2
20. Elidrissi B, Addou M, Regragui M et al (2001) Structure, composition and optical properties of ZnS thin films prepared by spray pyrolysis. Mater Chem Phys 68:175–179. https://doi.org/10.1016/S0254-0584(00)00351-5
21. López MC, Espinos JP, Martín F et al (2005) Growth of ZnS thin films obtained by chemical spray pyrolysis: the influence of precursors. J Cryst Growth 285:66–75. https://doi.org/10.1016/j.jcrysgro.2005.07.050
22. Hernández-Fenollosa MA, López MC, Donderis V et al (2008) Role of precursors on morphology and optical properties of ZnS thin films prepared by chemical spray pyrolysis. Thin Solid Films 516:1622–1625. https://doi.org/10.1016/j.tsf.2007.05.031

23. Zhu H, Huang JF, Wang Y et al (2011) Synthesis and characterisation of ZnS optical thin films through cathodic electrodeposition technique. Surf Eng 27:42–45. https://doi.org/10.1179/026708409X12490360426089
24. Kassim A, Ho SM, Abdul HA et al (2010) Influence of the depositio n time on the structure and morphology of the ZnS thin films electrodeposited on indium tin oxid e substrates. Dig J Nanomater Biostructures 5:975–980
25. Kim H, Moon JY, Lee HS (2012) Effect of ZnCl2 concentration on the growth of ZnO by electrochemical deposition. Curr Appl Phys 12:S35–S38. https://doi.org/10.1016/j.cap.2012.05.036
26. Moon JY, Kim H, Lee JH et al (2012) Synthesis of MgZnO nanostructures by electrochemical method. Curr Appl Phys 12:S52–S55. https://doi.org/10.1016/j.cap.2012.05.028
27. Benyahia K, Djeffal F, Ferhati H et al (2021) Microstructured ZnO-ZnS composite for earth-abundant photovoltaics: Elaboration, surface analysis and enhanced optical performances. Sol Energy 218:312–319. https://doi.org/10.1016/j.solener.2021.02.057
28. Azmand A, Kafashan H (2019) Al-doped ZnS thin films: physical and electrochemical characterizations. J Alloys Compd 779:301–313. https://doi.org/10.1016/j.jallcom.2018.11.268
29. Mosavi SM, Kafashan H (2019) Physical properties of Cd-doped ZnS thin films. Superlattices Microstruct 126:139–149. https://doi.org/10.1016/j.spmi.2018.12.002
30. Boosagulla D, Mandati S, Misra P et al (2021) Pulse electrodeposited zinc sulfide as an eco-friendly buffer layer for the cadmium-free thin-film solar cells. Superlattices Microstruct 160:107060. https://doi.org/10.1016/j.spmi.2021.107060
31. Bard AJ, Faulkner LR, White HS (2022) Electrochemical methods: fundamentals and applications. Wiley, Hoboken
32. Greef R, Peat R, Peter LM (1985) Electrocatalysis. Instrumental Methods in Electrochemistry. Oxford UK Albion Horwood Publication Ltd, Oxford, p 111
33. Djelloul A, Adnane M, Lerbah Y et al (2016) Élaboration et Caractérisation des Couches Minces de Sulfure de Zinc (ZnS) Préparés par la Technique SILAR (Successive Ionic Layer Adsorption and Reaction). Algerian J Res Technol 1:1–9
34. Hennayaka HMMN, Lee HS (2013) Structural and optical properties of ZnS thin film grown by pulsed electrodeposition. Thin Solid Films 548:86–90. https://doi.org/10.1016/j.tsf.2013.09.011